nagra
National Cooperative for the
Disposal of Radioactive Waste

TECHNICAL REPORT 02-21

Glass Dissolution Parameters: Update for Entsorgungsnachweis

June 2003

E. Curti

Paul Scherrer Institut, Villigen PSI

Hardstrasse 73, CH-5430 Wettingen/Switzerland, Telephone +41-56-437 11 11

nagra
National Cooperative for the
Disposal of Radioactive Waste

TECHNICAL REPORT 02-21

Glass Dissolution Parameters: Update for Entsorgungsnachweis

June 2003

E. Curti

Paul Scherrer Institut, Villigen PSI

Hardstrasse 73, CH-5430 Wettingen/Switzerland, Telephone +41-56-437 11 11

This report was prepared on behalf of Nagra. The viewpoints presented and conclusions reached are those of the author(s) and do not necessarily represent those of Nagra.

PREFACE

The Laboratory for Waste Management of the Nuclear Energy and Safety Research Department at the Paul Scherrer Institut is performing work to develop and test models as well as to acquire specific data relevant to performance assessments of planned Swiss nuclear waste repositories. These investigations are undertaken in close co-operation with, and with the financial support of, the National Cooperative for the Disposal of Radioactive Waste (Nagra). The present report is issued simultaneously as a PSI-Bericht and a Nagra Technical Report.

ISSN 1015-2636

ABSTRACT

This document provides updated long-term corrosion rates for borosilicate glasses used in Switzerland as a matrix for high-level radioactive waste. The new rates are based on long-term leaching experiments conducted at PSI and are corroborated by recent investigations. The asymptotic rates have been determined through weighted linear regressions of the normalised mass losses, directly calculated from B and Li concentrations in the leaching solutions. Special attention was given to the determination of the analytical uncertainty of the mass losses. The sensitivity of the corrosion rates to analytical uncertainties and to other criteria (e.g. the choice of data points for the regressions) was also studied. A major finding was that the uncertainty of the corrosion rate mainly depends on the uncertainty of the specific glass surface area. The reference rates proposed for safety assessment calculations are 1.5 mg m^{-2} d^{-1} for BNFL glasses and 0.2 mg m^{-2} d^{-1} for COGEMA glasses.

The relevance of the proposed corrosion rates for repository conditions is shown based on the analysis of processes and parameters currently known to affect the long-term kinetics of silicate glasses. Specifically, recent studies indicate that potentially detrimental effects, notably the removal of silica from solution through adsorption on clay minerals, are transitory and will not affect the long-term corrosion rate of the Swiss reference glasses. Iron corrosion products are also known to bind silica, but present data are not sufficient to quantify their influence on the long-term rate.

ZUSAMMENFASSUNG

Der vorliegende Bericht liefert aufdatierte Langzeitkorrosionsraten für Borosilicatgläser, die in der Schweiz als Matrix für hochradioaktive Abfälle dienen. Die neuen Raten basieren auf langfristigen, am PSI durchgeführten Auslaugexperimenten, und werden von kürzlich publizierten Untersuchungen bestätigt. Asymptotische Raten wurden durch gewichtete lineare Regressionen der normalisierten Massenverluste bestimmt, welche direkt aus B und Li Lösungskonzentrationen errechnet wurden. Besondere Aufmerksamkeit wurde der Ermittlung analytischer Unsicherheiten der Massenverluste gewidmet. Die Sensitivität der Korrosionsraten bezüglich analytischen Unsicherheiten und anderen Kriterien (z.B. die Auswahl der Datenpunkte für die Regression) wurde ebenfalls untersucht. Als Hauptfolgerung ergibt sich, dass die Unsicherheit der Korrosionsrate hauptsächlich vom Fehler der spezifischen Glasoberfläche abhängt. Die für die Sicherheitsanalyse vorgeschlagene Korrosionsraten sind 1.5 mg m^{-2} d^{-1} für BNFL-Gläser und 0.2 mg m^{-2} d^{-1} für COGEMA-Gläser.

Die Relevanz der vorgeschlagenen Korrosionsraten für Endlagerbedingungen wird anhand einer Analyse derjenigen Prozesse und Parameter aufgezeigt, die nach heutigem Kenntnisstand die Langzeitkinetik von Silicatgläsern beeinflussen. Insbesondere zeigen neue Studien, dass potentiell schädliche Effekte wie zum Beispiel die Adsorption von Kieselsäure an Tonmineralien vorübergehender Natur sind, und die Langzeitkorrosionsrate der Schweizer Referenzgläser kaum beeinflussen werden. Bekanntlich binden Eisenkorrosionsprodukte auch Kieselsäure, allerdings sind die gegenwärtigen Daten unzureichend, um deren Wirkung auf die Langzeitrate zu quantifizieren.

RIASSUNTO

Questo documento fornisce un aggiornamento dei tassi di dissoluzione a lungo termine dei vetri a borosilicato utilizzati in Svizzera come matrice per scorie ad alta radioattività. I nuovi tassi di corrosione si basano su esperimenti di lisciviazione a lunga durata eseguiti al PSI e sono confermati da recenti studi. I tassi asintotici sono stati determinati tramite regressioni lineari correlate delle perdite di massa normalizzate, direttamente calcolate dalle concentrazioni di Li e B nelle soluzioni. È stato dato peso particolare alla determinazione dell'incertezza analitica dei valori delle perdite di massa. Inoltre, si è studiata la sensitività dei tassi di corrosione agli errori analitici ed ad altri criteri (per esempio la scelta dei dati inclusi nelle regressioni). Un risultato fondamentale è che l'incertezza dei tassi calcolati dipende principalmente dall'errore dell'area specifica del vetro. I tassi di riferimento proposti per calcoli nell'ambito dell'analisi di sicurezza sono 1.5 mg m^{-2} d^{-1} per i vetri BNFL e 0.2 mg m^{-2} d^{-1} per i vetri COGEMA.

La rilevanza dei tassi proposti in condizioni di confinamento viene dimostrata tramite un'analisi dei processi e parametri che sulla base delle conoscenze attuali influiscono sulla cinetica a lungo termine dei vetri silicatici. In particolare, studi recenti indicano che effetti potenzialmente nocivi, ad esempio la rimozione della silice dalla soluzione per assorbimento su minerali argillosi, sono transitori e non influiranno sul tasso di corrosione a lungo termine dei vetri svizzeri di riferimento. È noto che pure i prodotti di corrosione del ferro fissano la silice, ma i dati attualmente disponibili sono insufficienti per quantificarne l'effetto sul tasso di corrosione a lungo termine.

RÉSUMÉ

Ce document fournit une mise à jour des taux de corrosion à long terme pour les verres à borosilicate utilisés en Suisse comme matrice des déchets hautement radioactifs. Les nouveaux taux sont basés sur des expériences de lixiviation à long terme conduites au PSI et sont confirmés par des travaux récents. Les taux asymptotiques ont été déterminés par des régressions linéaires corrélées des pertes de masse normalisées, calculées directement à partir des concentrations de B et de Li dans les solutions. Attention particulière a été apportée à la détermination de l'incertitude analytique des valeurs des pertes normalisées. En outre, on a étudié la sensitivité des taux de corrosion aux incertitudes analytiques et à d'autres critères (par exemple le choix des données inclues dans les régressions). Une conclusion fondamentale est que la précision des taux calculés dépend principalement de l'erreur de la surface spécifique du verre. Les taux de référence proposés pour les calculs d'analyse de sûreté sont 1.5 mg m^{-2} d^{-1} pour les verres BNFL et 0.2 mg m^{-2} d^{-1} pour les verres COGEMA.

La relevance des taux proposés en conditions de confinement est démontrée au moyen d'une analyse des processus et paramètres actuellement connus, influant sur la cinétique à long terme des verres à silicates. En particulier, des études récentes indiquent que des effets potentiellement néfastes, notamment la soustraction de silice de la solution par adsorption sur des minerais d'argile, sont transitoires et n'influeront pas sur le taux de corrosion à long terme des verres suisses de référence. Il est connu qu'aussi les produits de corrosion du fer lient la silice, mais les données actuellement disponibles sont insuffisantes pour en quantifier l'effet sur le taux à long terme.

TABLE OF CONTENTS

LIST OF FIGURES

LIST OF TABLES

1 INTRODUCTION

1.1 Background

This document provides updated dissolution rates for the two Swiss reference glasses resulting from reprocessed high-level radioactive waste. The update builds upon experimental and theoretical work performed in the last decade at PSI and in other European countries. Specifically, the results of the European Community project entitled "Experimental and modelling studies to formulate a source term of nuclear waste glass in representative geological storage conditions"[1] were considered in the update. The new glass corrosion rates were determined from ongoing long-term experiments started at PSI in December 1990. The improved precision of the kinetic data now available for the two reference glasses (COGEMA, France; and BNFL, U.K.) allows us to specify two distinct corrosion rates, whereas in the Kristallin-I safety assessment a unique rate was used for both glass types (NAGRA, 1994).

The report is structured as follows: Chapter 1 provides a brief overview of processes known to affect the kinetics of glass corrosion. It is intended to give background information on the kinetic models currently discussed in the community of glass corrosion science and to provide important clues to evaluate the relevance of the derived glass corrosion rates for repository conditions. Chapter 2 gives a summary of the long-term experiments carried out at PSI, from which the long-term rates for the two reference glasses have been derived. Brief descriptions of experimental procedures and results obtained up to date are presented. In addition, the procedure adopted for the selection of the new long-term rates is illustrated. Chapter 3 summarises the results of the above-mentioned European project, with emphasis on the effect of silica adsorption on glass dissolution rates. It is shown that this effect is not critical and does not reduce significantly the durability of vitrified waste under repository conditions. Finally, in chapter 4 updated reference rates for safety assessment calculations are given along with a short rationale of the method

[1] Program "Nuclear fission safety", EU-Nr. FI4W-CT95-0001, BBW-Nr. 95.0087, funded by the European Commission (EC) and the Federal Office for Education and Science (BBW).

used to define them. The report is completed by three appendices including the details of data evaluation as well as listings of raw experimental data and other derived quantities.

1.2 Processes affecting long-term rates

1.2.1 Preliminary remarks

This section provides a brief review of processes and parameters known to affect glass corrosion rates and an appreciation of the related uncertainties. The aim is to show that the use of the PSI long-term corrosion data to define reference rates for the safety analysis is justified, even if the measurements were carried out in the absence of engineered barrier materials like magnetite and bentonite. This review also provides a background for realistic parameter variations in the safety analysis. Finally, it is intended as a synopsis of current knowledge in glass corrosion science.

1.2.2 Silica concentration dependence

According to well-established empirical findings, the corrosion rate of borosilicate glasses depends on the dissolved silica concentration in the bulk solution. Since the rate appears to be inversely proportional to the dissolved silica concentration in the bulk solution, a first-order law has long been postulated to describe the dissolution kinetics of such glasses (GRAMBOW, 1984; GRAMBOW, 1985; VERNAZ & DUSSOSSOY, 1992). For a specific glass, the highest rate (the so-called "forward" rate[2]) is measured in pure water. At 90 ^{o}C it is in the order of 1 g m^{-2} d^{-1} for both Swiss reference glasses (WERME et al., 1990). As the Si solution concentration increases, the corrosion rate decreases down to a limiting minimum value, at which dissolved silica reaches a stationary concentration (the so-called "saturation" concentration). This minimum rate

[2] In the terminology of glass corrosion, the "forward" rate is the rate measured in pure water. The term is confusing since it suggests the existence of a "backward rate" of glass formation. Obviously, there is no backward rate since glass is thermodynamically unstable at the p,T conditions of interest.

corresponds to the "long-term" rate determined in chapter 2 and depends on glass composition. Typically, "forward" and "long-term" rates differ by 3-4 orders of magnitude. According to this model, the glass corrosion rate R [g m^{-2} d^{-1}] at any dissolved silica concentration C_{Si} below a theoretical limiting concentration C^* is defined by the following empirical equation (VERNAZ et al. 2001):

$$R = R_0 \left(1 - \frac{C_{Si}}{C^*} \right) \quad (1)$$

where R_0 is the glass corrosion rate in pure water ("forward" rate). Note that R_0 and C^* are purely empirical parameters that can be extrapolated from a series of rate measurements at different silica concentrations. C^* represents the theoretical concentration, at which glass corrosion would cease completely. However, according to the affinity model, C^* is never attained. Instead, a "saturation" concentration C_{sat} slighlty below C^* is reached, which is not exceeded at further reaction progress. This leads to a very small but measurable long-term rate R_∞:

$$R_\infty = \left(1 - \frac{C_{sat}}{C^*} \right) \quad (2)$$

The kinetics described by Eqs. (1) and (2) are attributed to the decreasing chemical affinity, i.e. to the decreasing difference between the chemical potentials of glass and solution, as silica and other glass components are progressively dissolved into the aqueous solution. Since glass is thermodynamically unstable at ambient conditions, a residual affinity, i.e. a small disequilibrium between glass and aqueous solution, persists indefinitely and the glass corrodes slowly until it is consumed (GRAMBOW, 1984; see also AAGARD & HELGESON, 1982).

1.2.3 The effect of protective gel layers

In recent years, the straightforward affinity model described above has been criticised by a group of French researchers, who proposed that the main cause of the rate decrease by 3-4 orders of magnitude is the formation of dense protective gel layers on top of the glass surface, not simply the increase in

dissolved silica concentration (see VERNAZ et al., 2001, and references therein). These authors point to experimental evidence showing that there is no glass-specific silica “saturation” concentration. For instance, different steady-state Si concentrations are obtained for the same glass as a function of S/V, a finding contradicting the simple affinity model. Furthermore, experiments carried out with pristine glass specimens put in contact with Si-rich solutions previously "saturated" with the same glass, showed initial rates much larger than the long-term rate expected when a pure affinity law is applied. On the other hand, the initial rates measured for pristine glass specimens in Si "saturated" solutions were significantly lower than the rates measured in pure water, indicating that the Si concentration in solution plays a role and cannot be simply ignored.

VERNAZ et al. (2001) came to the conclusion that the overall kinetics of borosilicate glasses are determined by the combined effect of Si concentration in the leachant and formation of protective gel layers. They state: "It is clear today that the effects of solution chemistry and of the protective gel properties are not contradictory, and must be considered together to account for experimental reality". The affinity law is thought to determine kinetics down to a reduction of the rate by a factor of ~ 5. At higher dissolved Si concentrations, silica polymerisation in the gel layer reduces the mobility of reactive species from and to the reactive glass surface. The release of B and Li thus decreases to the observed long-term values. Apparent silica diffusion coefficients as low as 10^{-19} m^2s^{-1} have been extrapolated for mature gel layers.

In summary, the processes governing glass corrosion kinetics and their interplay are not as simple as suggested by the first-order rate. They are still not understood in detail, and the debate about the relative importance of the affinity and diffusive terms is still open (see also GRAMBOW & MÜLLER, 2001).

1.2.4 Temperature dependence

The "forward" corrosion rate of borosilicate glasses is known to increase exponentially with temperature. Many glasses follow Arrhenius' law, with activation energies between 70 and 140 kJ/mol (LUTZE, 1988). For the MW

glass, an activation energy of ~ 80 kJ/mol could be determined from initial rate measurements between 70 and 110 ^{o}C (JSS-PROJECT, 1988), implying a reduction in rate by one order of magnitude for a decrease in temperature by ~30 ^{o}C. Unfortunately, an analogous effect, although probable, cannot be demonstrated for the long-term corrosion rate, due to the limited precision of kinetic measurements near Si "saturation" (JSS-PROJECT, 1988). The differences in the concentrations of B and Li after one year of corrosion as a function of temperature are within the precision of conventional analytical methods, i.e. they are too small to be detected. We therefore did not apply any temperature reduction for the reference long-term rates, in spite of the large temperature difference between laboratory experiments (90 ^{o}C) and HLW repository environment (~ 40 ^{o}C). The activation energy derived from "forward" rate measurements suggests long-term rates in the order of 10^{-4} g m^{-2} d^{-1} for BNFL glass and of 10^{-5} g m^{-2} d^{-1} for COGEMA glass at 60 ^{o}C. However, these rates are not supported by experimental results and remain thus speculative.

In contrast, "forward" corrosion rates can be safely extrapolated to about 60 ^{o}C on the base of reliable measurements conducted in the range 70 -110 ^{o}C (JSS-PROJECT, 1988). According to these data, the "forward" rate drops from 1 g m^{-2} d^{-1} at 90 ^{o}C to 0.1 g m^{-2} d^{-1} at 60 ^{o}C. The extrapolation to repository temperatures (~ 40 ^{o}C) is more uncertain due to lack of experimental data.

1.2.5 Sorption of Si on bentonite

It has been amply demonstrated that the presence of clays may lead to anomalously high glass corrosion rates (GODON, 1988, LEMMENS, 2001). This phenomenon was attributed to the decrease in dissolved silica concentration through adsorption on the clay (GODON, 1988; CURTI et al., 1993). Due to the coupling with the affinity law (Eq. 1), Si removal by sorption leads to higher corrosion rates, compared to systems without clay minerals or other Si sorbents. Application of this model with the highest partition coefficient for Si sorption on clays taken from the literature (TAN, 1982) had led to quite pessimistic forecasts for a generic repository environment (CURTI & SMITH, 1991). However, recent careful experiments (ADVOCAT et al., 1999) show that the distribution coefficients for Si adsorption on clays are much smaller than

those derived in some earlier studies (see chapter 3). The important spin-off is that the negative effects on the glass corrosion kinetics are smaller than previously assumed. Model calculations carried out with realistic distribution coefficients for Si (see ADVOCAT et al., 1999, and chapter 3 in this work) indicate that the fast glass corrosion kinetics induced by silica sorption is a temporary, short-term effect, with no significant influence on the release of most radionuclides. Nevertheless, it cannot be excluded that for short-lived, weakly-sorbing radionuclides ($t_{1/2} < 10^4$ y, e.g. ^{226}Ra) this transient phase of enhanced glass dissolution could lead to higher releases into the geosphere.

More recently, the detrimental effect of clays on the glass corrosion rate has been explained in terms of gel properties (VERNAZ et al., 2001, LEMMENS, 2001). Following this new interpretation (see section 1.2.3), silica removal through sorption on clay minerals would temporarily prevent the formation of a protective gel, thus delaying the attainment of the minimum long-term rate. This delaying effect would cease when the surface is saturated with sorbed silica.

A particularly unfavorable scenario has been pointed out by LEMMENS (2001). If precipitation of a secondary silicate, rather than sorption on the pre-existing clay, were the cause of silica removal, high corrosion rates could persist as long as such precipitates form. Thus precipitating silicates fixing the Si concentration at low levels would be particularly undesirable. This negative effect is demonstrably important in the case of Al-rich glasses, which promote formation of alumosilicates. It is much less pronounced in the case of the Al-poor borosilicate glass formulations like those used for the vitrification of Swiss high-level waste.

1.2.6 Effect of Fe corrosion products

Enhancement of the glass corrosion rate has also been observed in the presence of iron corrosion products. For instance, WERME et al. (1990) performed leaching experiments with COGEMA glasses in the presence of magnetite powder to simulate the effect of a corroded steel canister. Final corrosion rates after 1.5 years leaching time were significantly higher ($R \sim 0.05$ g m^{-2} d^{-1}) than those measured for similar experiments without

magnetite (R ~ 0.01 g m^{-2} d^{-1}). The authors interpreted this effect as due to "continuous slow formation of iron silicates or by multilayer sorption of silica on the surface of the iron corrosion products". The postulated process is thus similar to that proposed in the presence of clay minerals, and could in principle be modelled in a similar way as for sorption of silica on clay, as exemplified later in chapter 3.

However, a detailed inspection of the original data (JSS-PROJECT, 1987) revealed that the experiments of WERME et al. (1990) are not representative of long-term conditions. The experiments were conducted at very low S/V ratios (10 m^{-1}). Under such conditions, steady-state kinetics is not reached within 1.5 years, the longest reaction time of the experiments considered[3].

The results of WERME et al. (1990) are thus inconclusive and not suitable to determine long-term rates. Evidently, there is a general lack of experimental evidence on the effects of canister-glass interaction on glass corrosion. Additional experiments at higher S/V ratios and longer reaction times are needed to clarify the effect of iron corrosion products, as was done to elucidate the effect of clay minerals.

[3] In order to obtain long-term rates, leaching experiments are typically conducted at S/V of 1000 m^{-1} or higher. Silica “saturation" is then attained rapidly, enabling the determination of the asymptotic long-term rate. As evident from the parabolic form of the curves in Fig. 5 of WERME et al. (1990), their experiments had not reached steady-state conditions.

2 LONG-TERM LEACHING EXPERIMENTS

2.1 Experimental procedures and objectives

A series of long-term leaching tests were started in December 1990 at PSI's Waste Management Laboratory (LES). The main objective of the experiments was to obtain reliable and precise long-term corrosion rates for the two reference glasses used to solidify reprocessed radioactive high-level waste originating from Swiss nuclear power plants. Details of the experimental procedures are given in ZWICKY et al. (1992), here only a short summary is presented.

Powder samples from two inactive simulations of the two glass specifications (SON68 for the French COGEMA glass; MW for the British BNFL glass, see Table 2-1) were leached with distilled water in airtight stainless steel vessels at a constant temperature of 90 ^{0}C. The initial surface area to solution ratio was high (S/V = 1200 m^{-1}) in order to favour a rapid build-up of the dissolved Si concentration up to "saturation" conditions. Large amounts of glass powder (24 g) and water (600 mL) were used to enable repeated sampling of 10 mL aliquots without significantly disturbing the system. The experiments were carried out in quintuplet. After 5 years of reaction time, one of five experiments was interrupted for each glass type in order to obtain material for mineralogical analysis of the alteration products. The remaining experiments (two quadruplets) are still prosecuting; further data will be gathered within the GLASTAB project (5th RTD framework program funded by the European Community).

Table 2-1: Simplified composition of SON68 (COGEMA) and MW (BNFL) glasses, after ZWICKY et al. (1992).

Component (weight %)	SON68	MW
Al_2O_3	4.9	6.6
B_2O_3	14.0	16.0
CaO	4.0	~ 0
Fe_2O_3	2.9	3.1
Li_2O	2.0	3.9
MgO	~ 0	5.9
MoO_2	1.7	1.4
Na_2O	9.9	8.5
SiO_2	45.5	46.7
ZnO	2.5	~ 0
Other components*	12.6	7.9
Total	100.0	100.0

*mainly inactive isotopes or analogues of fission products and actinides

2.2 Determination of long-term corrosion rates

The amount of glass dissolved per unit exposed surface area ("normalised mass loss" $NL(i)$ [g m^{-2}]) is calculated from the solution concentrations of elements released congruently from the glass (typically B or Li), the exposed glass surface area, S [m^2], the element weight fraction in the fresh glass, f_i [-], and the solution volume, V [L]. Using the boron concentration, [B] [g / L], as a tracer of glass dissolution, the normalised mass loss is given by:

$$NL(B) = \frac{[B]}{f_B (S/V)} \quad . \tag{3}$$

The surface area is obtained by multiplying the measured specific surface area, ψ [m^2 g^{-1}], with the initial mass, m [g], of unaltered glass, while f_B can be readily

determined from the chemical analysis of the glass. In order to derive the long-term glass corrosion rate, R_∞ [g m^{-2} d^{-1}], the normalised mass loss, *NL(i)*, of congruently dissolving elements are plotted as a function of time. The rate is then determined from the asymptotic slopes of *NL(i)* vs. time plots (see Figures 2-1 and 2-2). Ideally, all elements that dissolve congruently should yield the same *NL(i)*-values and rates. The comparison of *NL(B)* and *NL(Li)*-values is thus an important consistency test.

In order to obtain reliable long-term rates, linear regressions were calculated from the asymptotic portion of the *NL(i)* vs. time plots (Figs. 2-1 and 2-2), taking account of the experimental uncertainties. In practice, only data for reaction times greater than 500 days were considered, while the data obtained at shorter times were excluded from the regression calculations. The resulting long-term rates are listed in Table 2-2. The details of the calculations, including the determination of *NL(i)* values, are given in Appendix A. Our evaluation indicates that the uncertainty of the long-term rates mainly depends on uncertainties in the exposed surface area, whereas other experimental errors play a minor role. Changes in the *S/V* parameter induced by the long corrosion times involved have been taken into account.

The reference rates proposed for safety assessment calculations (see chapter 4) correspond to the upper uncertainty limit of the mean rates reported in Table 2-2. The latter were determined directly from the slopes of the linear regressions for *NL(B)* or *NL(Li)* values (see Appendix A for more details). Note that the coincidence of rates derived from B and Li mass losses is a good indication for the internal consistency of the experimental data and supports the assumption of nearly congruent dissolution for these elements. The statistical precision justifies the selection of distinct rates for the two glasses. Previously (CURTI, 1991), it was not possible to discriminate between the two glasses due to the shorter reaction time of earlier leaching experiments (up to 1.5 years) so that a single rate (1.0×10^{-3} g m^{-2} d^{-1} = 3.8×10^{-4} kg m^{-2} a^{-1}) was used for both glasses in the Kristallin-I safety analysis (NAGRA, 1994).

An important issue is the question, whether it is justified to interpret the data with a linear regression model. As is evident from Figs. 2-1 and 2-2, a change

in slope occurs after 1500 days reaction time: after an initial phase of fast corrosion, the mean rate becomes almost zero in time span from ~500 to 1500 days; then a phase with apparently increased rate follows up to ~3000 days and finally the rates tend to vanish again. In order to answer this delicate question, the results of the regression analyses were evaluated with the help of statistical methods (Appendix A). Our conclusion is that the apparent changes in slope are not significant, since all *NL(i)*-values (± uncertainty) fall within the regression's uncertainty (see Figs. A1 and A2 in Appendix A). Hence, linear fits with a single corrosion rate for each dataset are appropriate, and there is no objective need to assume multiple rates during the time span of the leaching tests.

Table 2-2: Long-term glass dissolution rates for the MW and SON68 glasses calculated from B and Li normalised mass losses at reaction times ranging from 548 to 3650 days. The data of all ten experiments were considered in the regression calculations.

rates in [g m^{-2} d^{-1}]	rates (± σ) from *NL(B)*	rates (± σ) from *NL(Li)*
MW	9.6 (± 5.3) x 10^{-4}	6.8 (± 4.3) x 10^{-4}
SON68	1.3 (± 0.2) x 10^{-4}	1.3 (± 0.3) x 10^{-4}

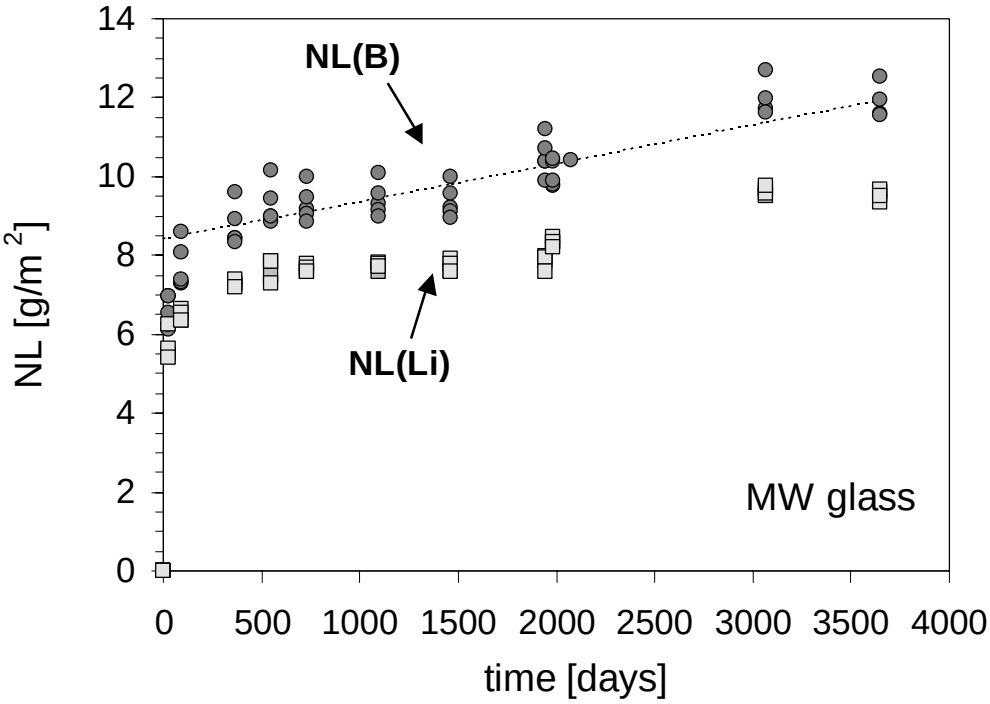

Figure 2-1: Normalised mass losses for the MW glass (BNFL) determined from boron and lithium concentrations in solution. The dotted line shows the linear regression through *NL(B)* data.

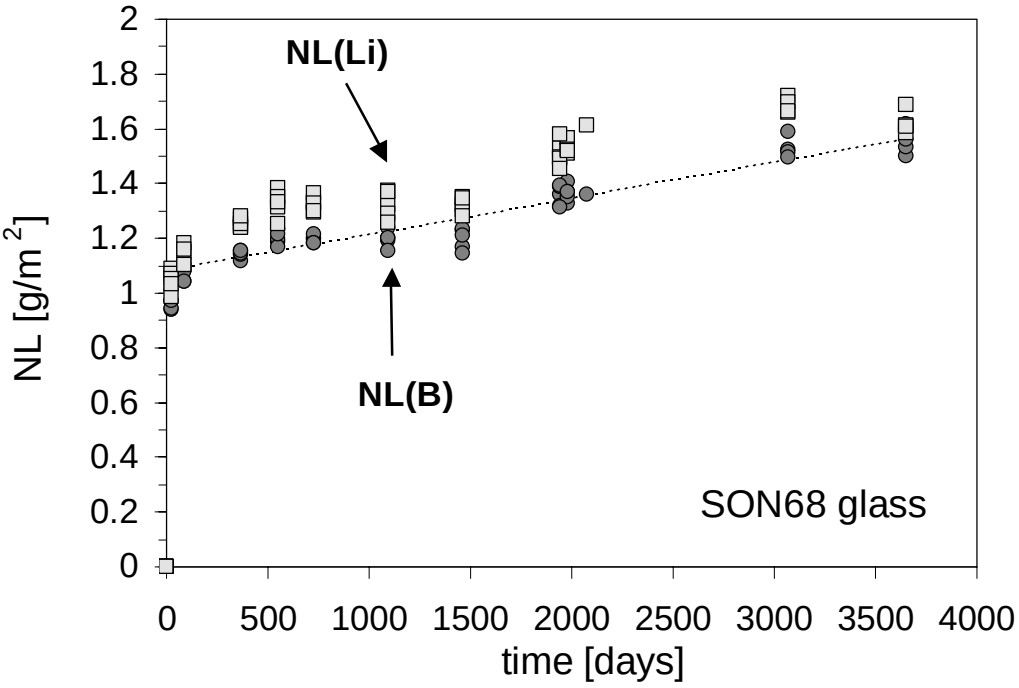

Figure 2-2: Normalised mass losses for the SON68 glass (COGEMA) determined from boron and lithium concentrations in solution. The dotted line shows the linear regression through *NL(B)* data.

2.3 Silica concentrations

Fig. 2-3 shows that the Si concentrations measured for the PSI long-term experiments (see also Tables C10-C11, Appendix C) are somewhat anomalous, since stationary concentrations are reached only after three years corrosion time. After the expected rapid increase in the first weeks, due to the very high specific surface area of 1200 m^{-1}, maximum silica concentrations between 100 -150 mg/L are attained at about one year corrosion time. This maximum is then followed by a decrease to stationary "saturation" concentrations of ~ 90 mg/L for both glasses. The temporary maximum can be explained by a kinetic effect, probably oversaturation with respect to a limiting silicate solid, which then slowly precipitates to reach thermodynamic equilibrium.

The later increase in Si concentrations measured for MW (and SON68 ?) solution samples at 2000 days reaction time correlates with a malfunction of the oven, which caused temporary cooling of the samples to ambient temperatures. The reasons for the renewed release of silica between 1500 and 2000 days are not well understood. It may be speculated that thermal stress induced by cooling could generate cracks, exposing fresh glass surfaces devoid of protective layers. The $NL(B)$ and $NL(Li)$ values apparently also increase during the same time span (Figs. 2-1 and 2-2) supporting this interpretation. However, as discussed in the preceding section and in Appendix A, the increase in B and Li concentrations is too small to be statistically significant.

A comparison of Fig. 2-3 with Figs. 2-1 and 2-2 shows that a simple affinity law (Eqs. 1 and 2) cannot be applied to these experiments at high Si concentrations. Indeed, the highest Si concentrations measured in the bulk solution do not correlate with the slowest rates. This is a clear indication in favour of a model combining the affinity law with the effects of a protective gel layer (see section 1.2.3).

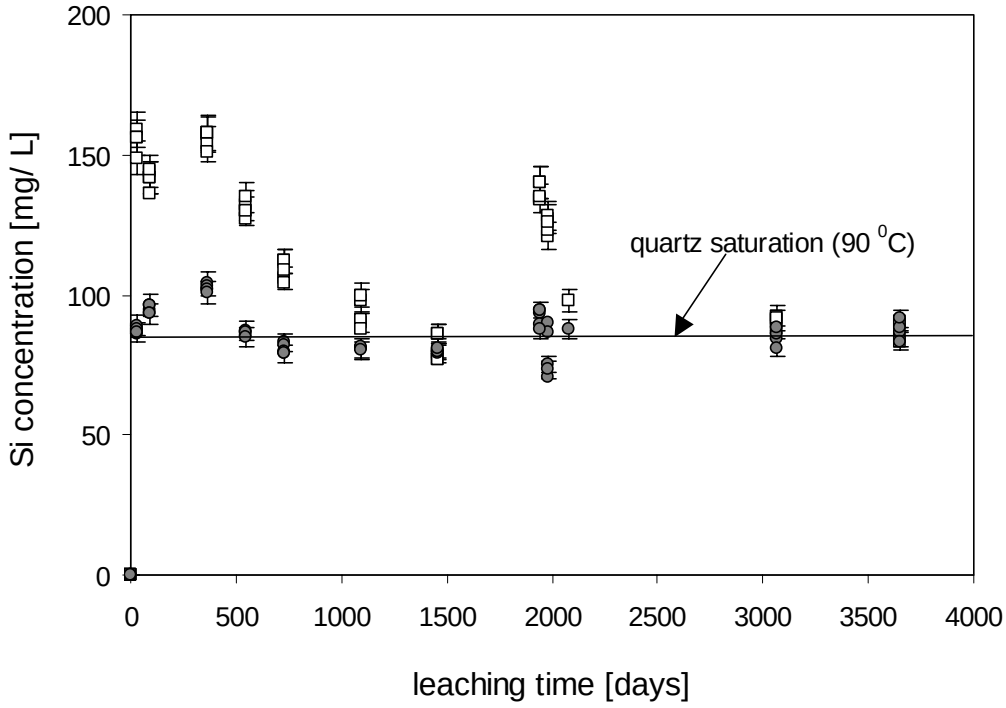

Figure 2-3: Si concentrations measured in sampled solutions in contact with MW (open squares) and SON68 (filled circles) glass powders, with corresponding analytical uncertainties. Centrifugation tests indicate that Si-colloids were absent in the sampled solutions. In the long term, a steady state concentration close to quartz saturation (~90 mg/L) is reached for both glasses. However, no quartz has been detected in the corrosion products up to date.

3 THE EFFECT OF CLAY-SILICA INTERACTION ON GLASS CORROSION KINETICS

3.1 Background

In the last years efforts have been made to assess the influence of host-rock and engineered barrier materials on glass corrosion. An important material in this respect is clay, a main component of backfill materials in many radioactive waste disposal systems. Early experiments carried out by GODON (1988) indicated that the French nuclear waste glass R7T7 degrades faster in the presence of smectite clay than in pure water. CURTI et al. (1993) interpreted this effect in terms of silica adsorption on clay mineral surfaces. The adsorption process is thought to reduce the silica concentration in the aqueous phase. Thus, according to the first-order rate law, which states that the glass dissolution rate is inversely proportional to the silica concentration (GRAMBOW, 1985; VERNAZ & DUSSOSSOY, 1992), the presence of silica-sorbing clays would lead to faster glass degradation, depending on the magnitude of the distribution coefficient of Si on the clay.

Model calculations performed assuming instantaneous reversible silica sorption on the clay suggested that this process could be detrimental in some repository situations, as it could considerably reduce the lifetime of vitrified waste (CURTI & SMITH, 1991). However, at that time studies on silica adsorption by clays produced widely different and contradictory results. Glass durability calculations performed with a conservative K_d-value of 0.5 m^3 kg^{-1} (TAN, 1982) led consequently to high glass corrosion rates and short lifetimes of the waste form.

This question was addressed in the project entitled "Experimental and modelling studies to formulate a source term of nuclear waste glass in representative geological storage conditions", carried out within the 4th RTD framework program funded by the European Commission. One objective was to define precisely the magnitude of Si sorption on relevant clay materials. To this aim, experiments were performed at CEA Marcoule in close cooperation with our laboratory, in order to determine the distribution coefficient for silica

adsorption on a smectite clay ("smectite 4a") and on a natural clay formation ("Boom Clay"). In a parallel study carried out by SCK-CEN (Belgium), K_d-values for Si were determined independently through batch and through-diffusion experiments (with the help of the radiotracer ^{32}Si). Details of these experimental studies are reported in ADVOCAT et al. (1999); below we give only a synthesis of the main results.

3.2 Measurement of silica adsorption on clays

The materials used were purified clay with high montmorillonite content ("smectite 4a") as analogue of a bentonite buffer, and samples from "Boom Clay", to represent a natural clay formation. The measured Si distribution coefficients are summarised in Table 3-1. Compared to the old literature values used in earlier model calculations (Table 3-2), the newly determined distribution coefficients for non-oxidised clays are smaller or comparable to those given by SIEVER & WOODFORD (1972), but 1-2 orders of magnitude smaller than those given by BECKWITH & REEVE (1963) and TAN (1982). Most important for the safety assessment, the distribution coefficient of 0.5 m^3/kg reported by TAN (1982) can be safely discarded, since this value appears exceedingly high compared to all other determinations.

Table 3-1: Comparison of silica sorption data (K_d / m^3 kg^{-1}) obtained in the context of the 4th European RTD Framework program (ADVOCAT et al., 1999). For a bentonite buffer, the values given for "smectite 4a" are relevant.

K_d for Si on clay materials / m^3 kg^{-1}	CEA-PSI (glass corrosion tests)	SCK-CEN (batch experiments)	SCK-CEN (^{32}Si through-diffusion experiments)
Smectite 4a	0.002 - 0.02	-	-
Boom clay (fresh)	0.002 - 0.05	0.02 - 0.03	0.005 - 0.01
Boom clay (oxidised)	-	0.03 - 0.1	-

Table 3-2: Distribution coefficients of silica for two montmorillonites and a bentonite derived from former literature data (CURTI et al., 1993).

Material	Leachant	pH	K_d / m^3 kg^{-1}	Reference
Montmorillonite	seawater	8.4 -9	0.018 - 0.148	SIEVER & WOODFORD (1972)
	distilled water	6-9	0.014 - 0.018	
Wyoming bentonite	distilled water	9	0.166	BECKWITH & REEVE (1963)
Montmorillonite	distilled water	7	0.5	TAN (1982)

3.3 The effect of silica adsorption on the durability of vitrified waste under repository conditions

On the base of the results given in Table 3-1, an upper K_d limit of 0.05 m^3 kg^{-1} for non-oxidised clay was selected[4]. This value was then used to model the effect of Si sorption on the durability of vitrified waste forms (see chapter 5.3.6 and Fig. 33 in ADVOCAT et al., 1999). The calculations were performed with the code GLADIS (CURTI & SMITH, 1991; CURTI et al., 1993), which couples silica sorption and diffusion with the rate equation for glass dissolution, assuming parameters reflecting the conditions and geometry of the planned Swiss repository. Specifically, calculations were performed at repository temperatures[5], resulting in a reduced "forward" rate (0.1 instead of ~ 1 g m^{-2} d^{-1}) and with a geometry consistent with the current repository design (cylindrical glass forms of 1.2 m axial length and 0.4 m diameter, surrounded by a 1.85 m thick layer of compacted bentonite). Glass fragmentation was accounted for by appropriately increasing the geometrical surface area of the glass forms by a factor of 12.5, as in the Kristallin-I safety analysis.

[4] Oxidised clay sorbs silica more strongly due to the presence of fine-grained Fe(III) iron oxides. These phases will however not form in a reducing repository.

[5] Instead of 90 °C, a temperature of 55 °C as for the KRISTALLIN-I safety assessment was assumed.

Fig. 3-1 shows the predicted effects of silica sorption on the performance of a R7T7 borosilicate glass matrix (corresponding to the SON68 glass) for two assumed distribution coefficients of silica on bentonite. These predictions are compared with an equivalent calculation where Si sorption is neglected. It is evident that only an exceedingly high sorption coefficient (0.5 m^3/kg) would have significant consequences. Specifically, in the initial phase of repository evolution (up to ~ 10'000 years after canister failure) glass degradation would proceed at least twice as fast as with realistic sorption parameters ($K_d \leq$0.05 m^3/kg). As already mentioned, a K_d of 0.5 m^3/kg correspond to the highest value ever reported in the literature, which has to be rejected in the light of the new data. The maximum expectable effect due to Si sorption is shown by the curve for K_d = 0.05 m^3/kg. The detrimental effect due to silica sorption is negligible in this case, and there is no significant reduction in the waste matrix lifetime. Even during the first 10'000 years the increase in corrosion would not exceed a few percent of the amount corroded in the absence of Si sorbent. These results indicate that silica sorption on clay minerals will not compromise the performance of borosilicate glass matrices within a repository.

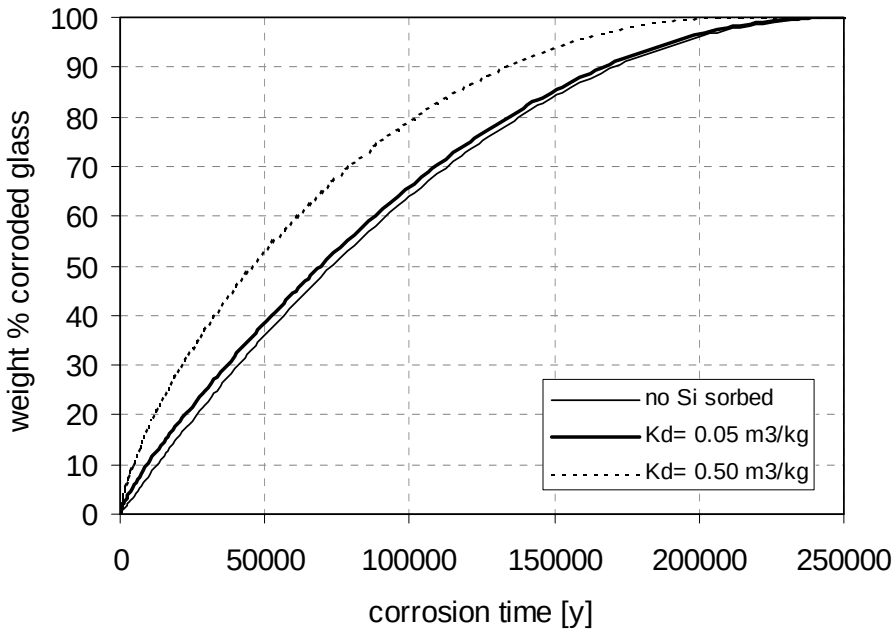

Figure 3-1: Effect of Si sorption by clay minerals on the performance of borosilicate waste forms in a repository environment. Calculations were performed with the GLADIS code, based on a parameter set optimised for conditions applying to a deep repository.

3.4 The effect of secondary silicate precipitation

According to LEMMENS (2001), the enhancement of glass corrosion kinetics in the presence of clay backfill materials could be due to secondary silicate precipitation rather than to adsorption. In this case the effect could persist indefinitely, as long as the precipitate forms.

The secondary precipitate could be either recrystallised backfill clay with a higher Si content than the original clay, or a separate, new silicate phase. In the case of the planned Swiss repository, the former possibility can be ruled out because the main mineral of the backfill material, montmorillonite, has the highest possible silica content. In montmorillonites, practically all tetrahedral sites are occupied by Si and there are no clay minerals with higher Si contents (NEWMAN, 1987).

In the long-term experiments described in this report, precipitation of secondary clay minerals was observed, even in the absence of bentonite backfill (CURTI et al., in prep.). Specifically, a layer of clay minerals (saponites or hectorites) formed on top of the MW glass surface. Similar clays, but in considerably smaller amounts, were observed in the altered SON68 glass. Our kinetic data indicate that the formation of these clays did not prevent the attainment of a residual rate 3-4 orders of magnitude lower than the initial rate. Moreover, contrary to the observations made by LEMMENS (2001) in the presence of Boom and FoCa clays, leaching tests carried out with ABS-118 glass (equivalent to SON68) in the presence of MX-80 bentonite did not indicate a significant enhancement of the corrosion rate (JSS-PROJECT, 1988; see also App. A in CURTI, 1991). This indicates that the observed rate effects are strongly dependent on the type of clay interacting with the glass and cannot be generalised.

4 UPDATE OF GLASS CORROSION PARAMETERS AND DISCUSSION

4.1 Criteria for the determination of reference rates

In this section, reference glass corrosion rates for the safety assessment "Entsorgungsnachweis 2002" are derived. As for the "Kristallin-I" safety analysis, we based our selection on state-of-the-art experimental data. The selected reference rates, given in Table 4-1, were thus derived from the long-term experiments described in section 2, following the procedure outlined in section 4.2.

Corrosion rates extrapolated from natural analogue studies, e.g. studies on the alteration of volcanic glasses in seawater or meteoric water, have not been considered for the determination of long-term corrosion rates. Attempts to derive corrosion rates from the thickness of the alteration layer in submarine basaltic glasses yielded widely different results, with inferred rates varying within five orders of magnitude (GRAMBOW et al., 1986). This inconsistent picture is probably the result of variable boundary conditions during these "natural experiments". For instance, contact times with the leaching solution are not known, since the age of the rock is not necessarily identical with the duration of water/rock interaction. Even within a sample, the thickness of the alteration layer may vary considerably, reflecting different times of water/rock interaction. Moreover, the chemistry of volcanic glasses differs considerably from that of nuclear waste glasses, so that the results inferred from these natural analogues cannot be directly transferred to borosilicate glasses.

On the other hand, natural analogues are valuable tools in estimating the long-term mineralogical evolution of glasses. The study of volcanic glasses altered in seawater or subglacial freshwater can give important clues on the nature of potential host phases for radionuclide immobilisation. Previous studies indicate that the final stable products of alteration are clay minerals and zeolites, which can incorporate a number of radionuclides (HONNOREZ, 1978; DAUX et al., 1994).

4.2 Definition of reference rates

Best estimates for the long-term corrosion rates of the COGEMA and BNFL reference glasses in pure water at 90 ^{o}C have been derived as follows from the data collected for the long-term experiments:

a) Calculation of B and Li normalised mass losses, $NL(i)$ [g m^{-2}], from the measured solution concentrations according to (Eq. 3).

b) Calculation of a linear regression through the $NL(i)$ values for times larger than 500 days, yielding best-fit rates with statistical uncertainties.

c) Selection of the higher of the two mean rates obtained from B or Li normalised mass losses (see Table 2.2).

Reference rates for safety assessment calculations have then been defined as the sum of best estimates plus the corresponding uncertainty (i.e. reference rate = best-estimate rate + σ, as given in Table 2.2, rounded to 10^{-4} g m^{-2} d^{-1}). This procedure yielded the values reported in Table 4.1.

Table 4-1: Updated reference glass corrosion rates for safety analysis calculations.

	BNFL glass (MW)	COGEMA glass (SON68)
R_{∞} [g m^{-2} d^{-1}]	1.5 x 10^{-3}	2 x 10^{-4}
R_{∞} [kg m^{-2} a^{-1}]	5.5 x 10^{-4}	7.3 x 10^{-5}

REFERENCES

AAGARD, P., HELGESON, H.C. (1982), "Thermodynamic and kinetic constraints on reaction rates among minerals and aqueous solutions. I. Theoretical considerations". Am. J. Sci. **282**, pp. 237-285.

ADVOCAT, T., et al. (1999), "Experimental and Modeling Studies to Formulate a Nuclear Waste Glass Source Term in Representative Geological Disposal Conditions- FINAL REPORT", Technical Report RT/DRRV/N°99.11 (final report of EU project FI 4W CT950001) CEA-Valrho, Marcoule, Bagnols-sur-Ceze.

BECKWITH R.S. & REEVE R. (1963) "Studies of soluble silica in soils - I. The sorption of silicic acid by soils and minerals", Aust. J. Soil Res. 1, pp. 157-168.

BEVINGTON P.R. (1969) "Data reduction and error analysis for the physical sciences". McGraw-Hill, New York, 336 p.

CURTI, E. (1991). "Modelling the dissolution of borosilicate glasses for radioactive waste disposal with the PHREEQE/GLASSOL code: theory and practice", PSI-Report Nr. 86, Paul Scherrer Institut, Villigen, Switzerland, and Technical Report NTB 91-08, NAGRA, Wettingen, Switzerland.

CURTI, E. & P.A. SMITH (1991). "Enhancement of borosilicate glass dissolution by silica sorption and diffusion in compacted bentonite: a model study". In: *Scientific Basis for Nuclear Waste Management XIV*, Mat. Res. Soc. Proc. 212, pp. 31-39, Boston: Materials Research Society (1991).

CURTI, E., GODON N., & VERNAZ E.Y. (1993) "Enhancement of the glass corrosion in the presence of clay minerals: testing experimental results with an integrated glass dissolution model". In: *Scientific Basis for Nuclear Waste Management XVI*, Mat. Res. Soc. Proc. 294, pp. 163-170, Boston: Materials Research Society.

CURTI, E., CROVISIER J.-L., & KARPOFF, A.M. (in prep.) "Secondary mineral formation during long-term alteration (13 years) of two simulated nuclear waste glasses (SON68, MW)".

DAUX, V.,CROVISIER J-L., HEMOND C. & PETIT J.C.(1994) "Geochemical evolution of basaltic rocks subjected to weathering: fate of major elements, rare earth elements and thorium", Geochim. Cosmochim. Acta, 58, pp. 4941-4954.

GODON, N. (1988) "Effet des matériaux d'environnement sur l'altération du verre nucléaire R7T7 - influence des argiles", Ph. D. thesis, Univ. Orléans, France.

GRAMBOW, B. (1984) "Ein physikalisch-chemisches Modell für den Mechanismus der Glaskorrosion - unter besonderer Berücksichtigung simulierter radioaktiver Abfallgläser." Ph. D. Thesis, Freie Universität Berlin, 255 p.

GRAMBOW, B. (1985) "A general rate equation for nuclear waste glass corrosion". In: *Scientific Basis for Nuclear Waste Management VIII*, Mat. Res. Soc. Proc. 44, pp.15-27, Boston: Materials Research Society.

GRAMBOW, B., JERCINOVIC, M.J., EWING, R.C. & BYERS, C.D. (1986) "Weathered basalt glass: a natural analogue for the effects of reaction progress on nuclear waste glass alteration". In: *Scientific Basis for Nuclear Waste Management IX*, Mat. Res. Soc. Proc. 50, pp. 263-272, Boston: Materials Research Society.

GRAMBOW, B., & MÜLLER, R. (2001) "First-order dissolution rate law and the role of surface layers in glass performance assessment" J. Nucl. Mat. **298**, pp. 112-124.

HONNOREZ, J. (1978) "Generation of phillipsites by palagonitization of basaltic glass in seawater and the origin of K-rich deep sea sediments" In: *Natural Zeolites, Occurrence, Properties, Use*, S.B. Sand and F.A. Mumpton, eds., Pergamon, Oxford, pp. 245-258.

JSS-PROJECT (1987) "Experimental and modeling studies of HLW glass dissolution in repository environments" Technical Report JSS 87-01, Swedish Nuclear Fuel and Waste Mangement Co. (SKB), Stockholm.

JSS-PROJECT (1988) "Testing and modelling of the corrosion of simulated nuclear waste glass powders in a waste package environment" Technical Report JSS 88-02, Swedish Nuclear Fuel and Waste Mangement Co. (SKB), Stockholm.

LEMMENS, K. (2001) “The effect of clay on the dissolution of nuclear waste glass”. J. Nucl. Mat. **298**, pp. 11-18.

LUTZE, W. (1988) "Silicate glasses". In: Radioactive waste forms for the future, W. Lutze and R.C. Ewing, eds., North-Holland, Amsterdam, pp. 1-159.

NAGRA (1994) "Kristallin I - Safety assessment report" Technical Report NTB 93-22, NAGRA, Wettingen, Switzerland.

NEWMAN, A.C.D. (1987) "Chemistry of clays and clay minerals”. Longman, 480 p.

PRESS, W.H., FLANNERY B.P., TEULKOLSKY S.A. & VETTERLING, W.T. (1989) "Numerical Recipes - The Art of Scientific Computing (FORTRAN Version), Cambridge University Press, Cambridge (U.K.), pp. 498-509.

SIEVER, R. & WOODFORD, N. (1973) "Sorption of silica by clay minerals", Geochim. Cosmochim. Acta, 37, pp. 1851-1880.

TAN K.H. (1982) "The effect of interaction and adsorption of silica on structural changes in clay minerals", Soil Sci. 134, pp. 300-307.

VERNAZ, E.Y. & DUSSOSSOY J.L. (1992) "Current state of knowledge of nuclear waste glass corrosion mechanisms: the case of R7T7 glass", Applied Geochemistry, Suppl. Issue No. 1, pp. 13-22.

VERNAZ, E.Y., GIN, S., JÉGOU, C. & RIBET, I. (2001) "Present understanding of R7T7 glass alteration kinetics and their impact on long-term behavior modeling", J. Nucl. Mater. **298**, pp. 27-36.

WERME, L., BJÖRNER, I.K., BART, G., ZWICKY H.U., GRAMBOW, B., LUTZE, W., EWING, R.C. & MAGRABI, C. (1990) "Chemical corrosion of highly radioactive borosilicate nuclear waste glass under simulated repository conditions", J. Mater. Res. **5** (5), pp.1130-1146.

ZWICKY H.U., GRABER TH. & KEIL R. (1992) "Versuche zur Bestimmung der Langzeitkorrosionsrate von Alkaliborosilicatglas: Zwischenbericht". Technical Report TM-43-92-26, Paul Scherrer Institut, Villigen, Switzerland.

ACKNOWLEDGEMENTS

Many thanks are due to Stéphane Gin (CEA) and his colleques for their careful review. My collegues Urs Berner and Wolfgang Hummel (PSI) as well as Bernhard Schwyn (Nagra) are gratefully acknowledged for their suggestions and constructive criticism.

APPENDIX A: DETERMINATION OF LONG-TERM CORROSION RATE AND RELATIVE UNCERTAINTY

A.1 Calculation of normalised mass losses and uncertainties

The rate of glass dissolution, R [m^2 g^{-1} d^{-1}] can be calculated from a series of concentration measurements for a congruently dissolving element i at different reaction times. Congruent dissolution implies that the element in question is dissolved quantitatively from the glass network, without being trapped in secondary solid nor sorbed on any surface. Normally, only very soluble elements like B and Li fulfill such stringent conditions. In a first step the normalised mass losses, $NL(i)$ [g m^{-2}], of a congruently dissolving element are determined. Using boron as a tracer of the glass dissolution process, the normalised mass loss is given by:

$$NL(B) = \frac{[B]}{f_B (S/V)} \qquad \text{(A1)}$$

where $[B]$ is the solution concentration [g/L], f_B is the weight fraction of boron in the unaltered glass [g of boron / g of glass], S is the water-exposed surface area [m^2], and V [L] is the solution volume. Similar expressions can be derived for all other elements present in the glass. The quantity f_B can be determined from the formulation or chemical analysis of the unaltered glass, while $[B]$ and V are measured by standard analytical techniques. The surface area cannot be measured directly. It can, however, be evaluated from the specific surface area, ψ [m^2 g^{-1}], and the mass, m [g], of unaltered glass.

If all elements were dissolved congruently, all $NL(\mathrm{i})$ values would be identical and equal to the net amount of glass dissolved per unit exposed surface area. In practice, most elements (e.g. Si, Al, Ca, Fe) dissolve incongruently, since important fractions of them are retained in the residual gel layer formed by the corroding glass or in secondary products precipitated on top of the glass surface. For these elements, $NL(i)$ values are lower than for elements dissolved

congruently, quantifying the extent of retention in the gel layer or in the corrosion products.

The long-term corrosion rate is defined by the asymptotic slope in a plot of $NL(B)$ or $NL(Li)$ as a function of reaction time (see Figures 2-1 and 2-2):

$$R_{\infty}(B) = \frac{dNL(B)}{dt} . \qquad \text{(A2)}$$

In order to obtain a reliable value of the long-term rate, a linear regression accounting for the uncertainties affecting all the quantities in the right-hand side of Eq. (A1) must be calculated. Except for f_B, all other quantities are in principle time dependent: V decreases due to the repeated solution sampling, while [B], ψ and m (and consequently S) change due to the progress of the glass corrosion process.

Calculations were performed with a simple geometric model to predict the change in surface area as a function of corrosion time (Appendix B). These indicate only a small variation of the (S/V) ratio for the experiments with MW glass powder, although the total mass loss over 10 years was ~30 % of the initial glass amount. With increasing corrosion time, the reduction in surface area is compensated by the decrease in solution volume due to solution sampling (Table C8, Appendix C). In contrast, in the experiments conducted with SON68 glass the decrease in surface area is minor (only 4% of the initial glass), but since the solution volume decreases significantly due to repeated sampling, a net increase of ~20% in the (S/V) ratio is calculated. These effects, although minor, were taken into account in calculating $NL(B)$ and $NL(Li)$ values from the SON68 experimental data and were therefore not included in the calculation of the uncertainty for the latter quantity. In contrast, $NL(B)$ and $NL(Li)$ values for the MW glass were calculated assuming a constant (S/V) of 1200 m^{-1}, considering that the difference between initial and final values is less than 10%.

Table A1: Uncertainties in the measured quantities affecting the normalised mass losses.

Variable	Relative uncertainty $(\sigma_y / y) \times 100$	Remarks
$[B]$	± 2 %	from analytical deviations in the concentrations of internal solution standards
$[Li]$	± 5 %	idem
V	± 1 %	estimated assuming an error of 0.5% in the initial volume measurement and 2% in the successive samplings (10 mL each)
f_B	± 2 %	from variations in glass analyses, see p. 4 in ZWICKY et al. (1992)
f_{Li}	± 2 %	idem
S	± 30 % (MW) ± 10 % (SON68)	from variation of surface area measurements (see JSS-PROJECT, 1988, p. 12 and Appendix B)

The normalised mass losses calculated for B and Li are given in Appendix C (Tables C5-C8) along with the measured solution concentrations (Table C1-C4) and the calculated S/V ratios (Table C9). The overall relative uncertainty affecting NL-values was estimated using simple error propagation formulae (BEVINGTON, 1969, p. 60) with the uncertainties as specified in Table A1.

The approximate relative standard deviation for normalised mass losses calculated from boron concentrations is given by:

$$\frac{\sigma_{NL_B}}{NL_B} = \sqrt{\left(\frac{\sigma_{[B]}}{[B]}\right)^2 + \left(\frac{\sigma_{f_B}}{f_B}\right)^2 + \left(\frac{\sigma_V}{V}\right)^2 + \left(\frac{\sigma_S}{S}\right)^2} \qquad \text{(A3)}$$

$$= \sqrt{0.02^2 + 0.02^2 + 0.01^2 + 0.3^2} \cong \pm 30\ \%$$

The numbers used in Eq. (A3) are for the MW glass experiments and illustrate that the overall uncertainty is dominated by the uncertainty in the exposed surface area. The resulting relative uncertainties of NL-values used in the regression analysis are given in Table A2.

Table A2: Calculated uncertainties (100 x σ_{NL} / NL) of normalised mass losses, determined with Eq. (A3) using the standard deviations given in Table A1.

	MW glass	SON68 glass
NL_B	30 %	10 %
NL_{Li}	30 %	10 %

A.2 Calculation of linear regressions and uncertainties

The results of the linear regression analyses used to determine the long-term corrosion rates are given in Table A3. The linear fits were calculated with the χ^2-minimisation method following the treatment of PRESS et al. (1989), described in detail below. The long-term corrosion rates with corresponding uncertainties, reported in chapter 2, are given directly by the slopes of these regression lines.

Table A3: Results of linear regression analyses of *NL(Li)* and *NL(B)* values as a function of reaction time, performed with the χ^2-minimisation method (routine "FIT" in PRESS et al., 1989). In order to determine the asymptotic slope (yielding the long-term rate) only data at times larger than 500 days were included in the regressions. For each of the two glasses (MW and SON68) glasses, the data of all five experiments were combined to yield single regression lines.

	MW glass		SON68 glass	
	NL(B)	*NL(Li)*	*NL(B)*	*NL(Li)*
input:				
number of points[1]	39	39	39	39
uncertainty[2]	± 30 %	± 30 %	± 10 %	± 10 %
output:				
slope[3] [g m^{-2} d^{-1}] x 10^{-4}	9.62 ± 5.32	6.81 ± 4.30	1.31 ± 0.23	1.29 ± 0.27
intercept[4] [g m^{-2}]	8.43 ± 0.97	6.99 ± 0.79	1.09 ± 0.04	1.22 ± 0.05
χ^2 (chi-square)[5]	1.04	0.56	4.21	7.00

[1] data reported in Tables C5 to C8
[2] see Table A2
[3] corresponds to long-term rate
[4] has no practical meaning
[5] gives a measure of the deviation of the data from the statistical model. Good fits correspond to values of less than 2. The very low χ2 values for MW-regressions probably indicate some overestimation of data uncertainty.

A.3 Robustness of calculated regressions

An important question to address, is whether the apparent changes in slope observed in the course of the experiments are statistically significant. To answer this question, it is necessary to know some details about the statistical model used to calculate the best-fit lines and the uncertainties of the regression parameters (i.e. intercept and slope). The method is described in detail in PRESS et al. (1989). Here, only the points relevant for the present discussion are given.

Since in each regression equal uncertainties are assumed for all data points (σ_I = constant), χ^2-minimisation yields always the same best-fit line, independent of the magnitude of the experimental uncertainty σ_i assigned to each point. This is evident when the equations defining a and b (Eq. 14.2.6 in PRESS et al., 1989) are solved for a constant value for σ_i. Then σ_i cancels out, yielding:

$$a = \frac{\Sigma x_i^2 \ \Sigma y_i - \Sigma x_i \ \Sigma(x_i, y_i)}{N \ \Sigma x_i^2 - (\Sigma x_i)^2} \tag{A4}$$

$$b = \frac{N \ \Sigma(x_i, y_i) - \Sigma x_i \ \Sigma y_i}{N \ \Sigma x_i^2 - (\Sigma x_i)^2} \tag{A5}$$

where (x_i,y_i) are the individual points in the regression, N is the total number of data points and Σ stays for the summation over the N data points. Therefore, the values of intercept, a, and slope, b, will be always the same, regardless of the magnitude of σ_i. In contrast, the uncertainties σ_a and σ_b of the calculated intercept and slope **do** depend on the data uncertainty σ_i . Solving Eq. 14.2.9 in PRESS et al. (1989) with a constant value for σ_i leads to:

$$\sigma_a = \sigma_i \sqrt{\frac{\Sigma x_i^2}{N \ \Sigma x_i^2 - (\Sigma x_i)^2}} \tag{A6}$$

$$\sigma_b = \sigma_i \sqrt{\frac{N}{N \Sigma x_i^2 - (\Sigma x_i)^2}} \tag{A7}$$

This means that the uncertainty associated to intercept and slope will increase proportionally with the uncertainty assigned to the data.

Figure A1 shows for the SON68 experiments a comparison of the NL-data with the regression model, showing the best fit ($y = a + b\,x$) as continuous line. The uncertainty of the best fit is defined by the two limiting broken lines. These were calculated taking into account the uncertainty of the regression, i.e. $y = (a \pm \sigma_a) + (b \pm \sigma_b)\,x$. The plots show that all the data fall (within their uncertainty) in the

field defined by the two broken lines, both for the $NL(B)$ and $NL(Li)$ regression. **Hence, we conclude that the apparent change in slope observed between 1500 and 2000 days is statistically not significant and that a model with a single linear regression is justified**. Note that the latter conclusion is permissible only because the regression uncertainty depends uniquely on the experimental errors associated to the fitted data and is not determined by the scattering of the NL-data (the latter procedure being used when experimental errors are unknown). Hence, data and regression uncertainty are independent of each other. Similar conclusions can be reached for the MW-data (Figure A2): even assuming the lower error limit for NL-values (10% instead of 30%), all the data fall (within their uncertainty) in the uncertainty field of the regression.

If the experimental data had a better precision (of, say, $\pm$ 3%) then a lower uncertainty of the regression would result. As a consequence, some of the points would lie outside the field defined by the regression uncertainty. It would no longer be justifiable to model the data with a single linear regression. Alternative models with multiple linear rates or a functional variation would be required instead of a single asymptotic corrosion rate.

Two questions remain, which need some attention. Firstly, the selection of the minimum corrosion times to be included in the regressions. In the previous linear regressions, only data at reaction times > 500 days were selected. However, this choice is somehow arbitrary, since that the data at 365 days and even 91 days could in principle also be included, as evident from Figures A1 to A3. Secondly, the effect of neglecting the variation of S/V in calculating $NL(B)$ and $NL(Li)$ for the MW glass experiments has not be explored.

In order to study the consequences of our choice to use only data > 500 days and to disregard variations in (S/V), we performed two alternative regression calculations for the MW data. The first takes into account the (S/V) correction, the second additionally includes the data collected at 365 days. It is clear from the results listed in Table A4 that only minor differences in the calculated rates result from the alternative data treatment.

Table A4: Results of alternative linear regression analyses for MW data (see text for details).

	rate [g m^{-2} d^{-1}] x 10^{-4}		intercept [g m^{-2}]	
	NL(B)	*NL(Li)*	*NL(B)*	*NL(Li)*
S/V =constant (ref.case)	9.6 ± 5.3	6.8 ± 4.3	8.4 ± 1.0	7.0 ± 0.8
S/V variation considered	8.6 ± 5.4	6.1 ± 4.4	8.9 ± 1.0	7.4 ± 0.8
365 days data included	9.0 ± 4.8	4.3 ± 4.0	8.8 ± 0.8	7.8 ± 0.4

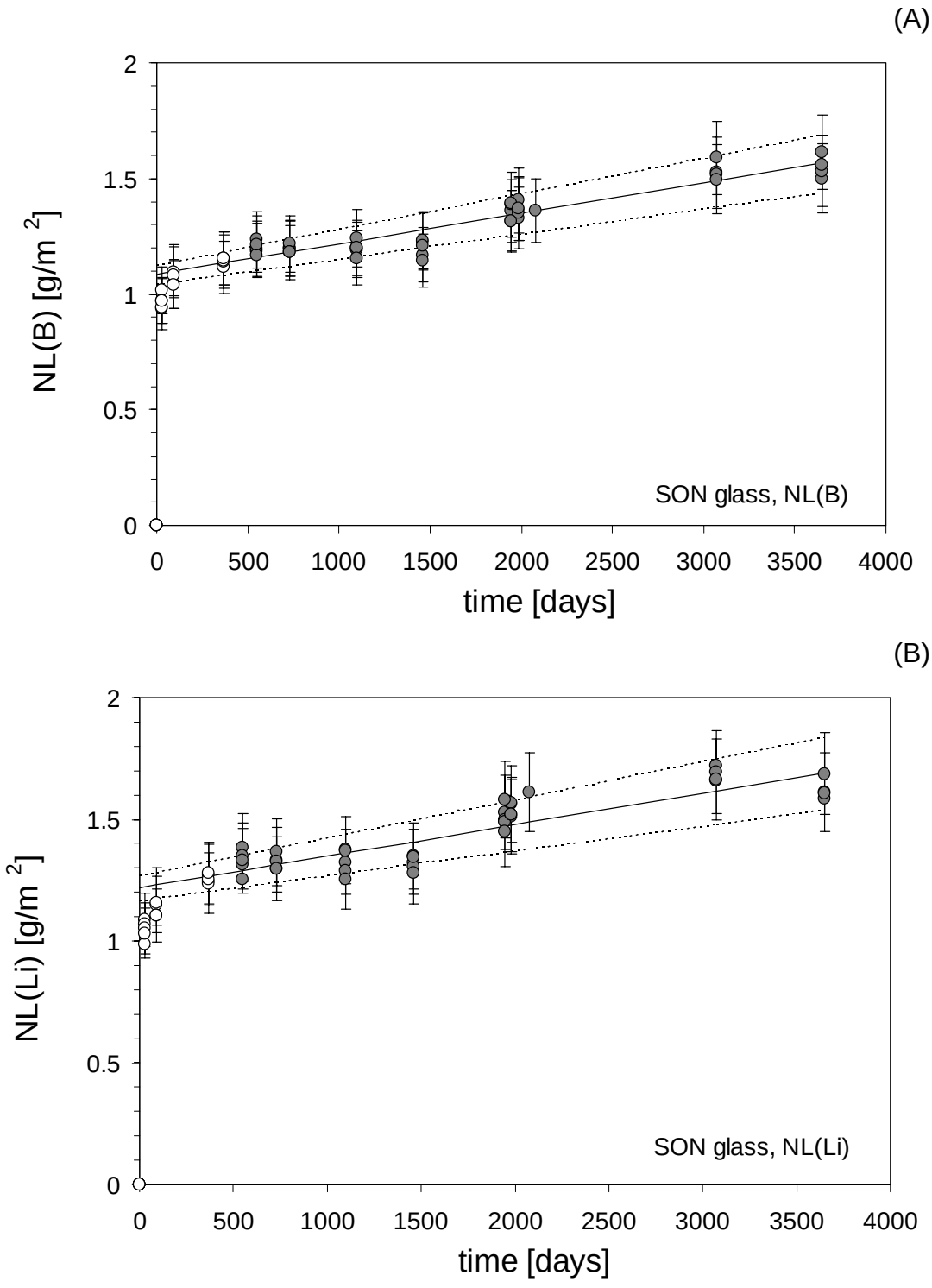

Figure A1: Comparison of data and statistical model for SON68 glass experiments. Filled circles represent data included in the regression; open circles represent transient data prior to "saturation" conditions. The solid line represents the best fit; broken lines delimit the uncertainty of the fit ($\pm \sigma$ =10 %).

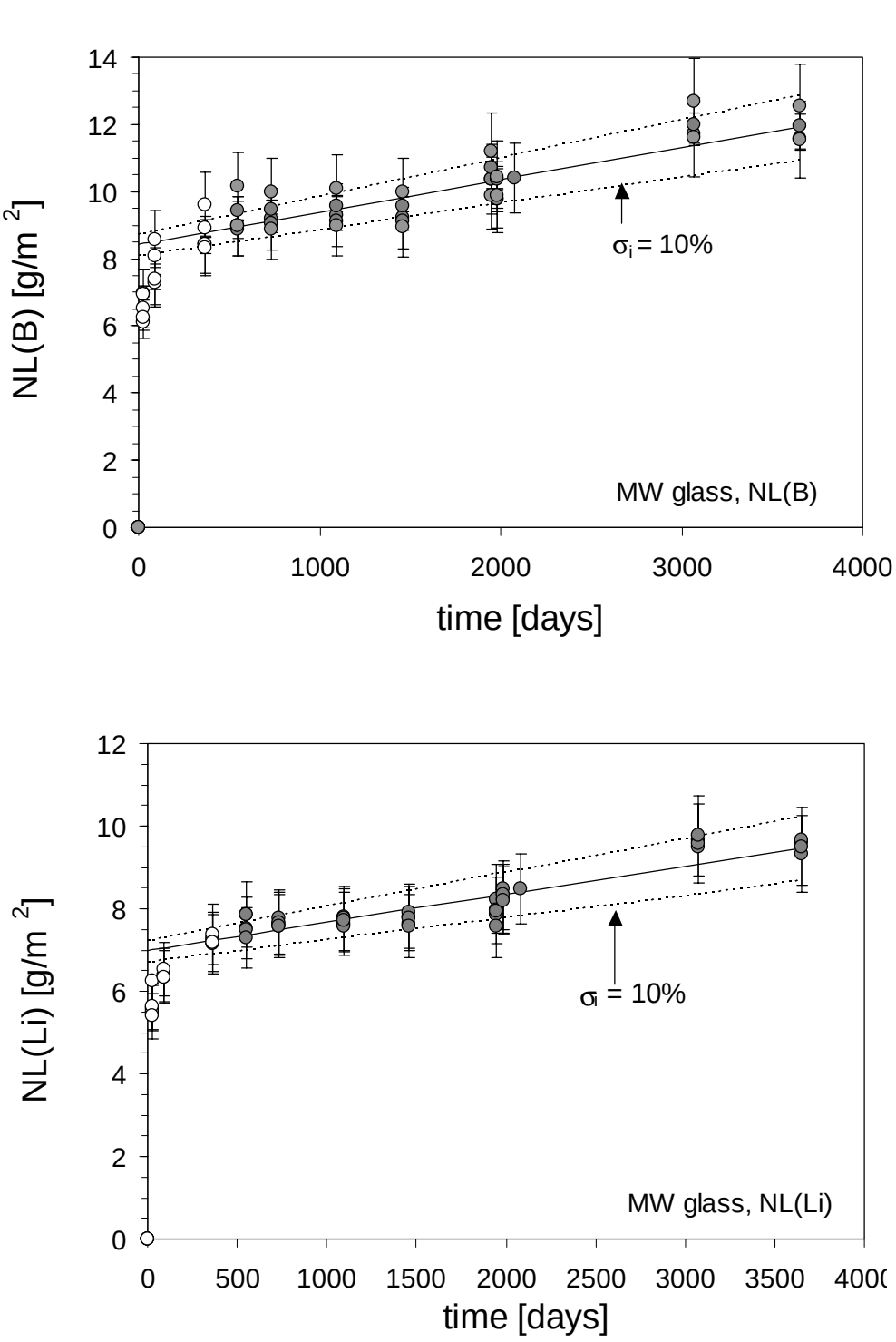

Figure A2: Comparison of data and statistical model for MW glass experiments. Filled circles represent data included in the regression; open circles represent transient data prior to "saturation" conditions. The solid line represents the best fit; broken lines delimit the uncertainty of the fit ($\pm \sigma$ =10 %).

APPENDIX B: VARIATION AND UNCERTAINTY OF THE (S/V) RATIO

B.1 Introductory remarks

Both surface area and solution volume change in the course of the glass corrosion experiments. The initial volume of 0.6 L decreases due to the repeated sampling (10 mL) of solution for analysis, while the exposed surface area changes due to the progress of the corrosion reaction. While changes in solution volume can be monitored precisely, variations of the exposed surface area are difficult to predict, as they depend on several uncontrollable factors like surface roughness, grain geometry and permeability of the alteration layer. Consequently, among the experimental quantities affecting the calculation of normalised mass losses (see Eq. 3) the surface area is the most uncertain.

There are two main sources of uncertainty that need to be considered in view of the determination of the long-term rate:

a) uncertainties deriving from measurements of the initial specific surface area, S_o*:* Stereoscopic and BET measurements on both glass powders were performed in two different laboratories (PSI and Studsvik, see JSS-PROJECT, 1988, p. 12) on separate batches, prepared with slightly different procedures. Stereoscopic analyses yielded consistent values (0.03 ± 0.002 m^2g^{-1}) for both glasses in both laboratories. In contrast, BET measurements led to considerable interlaboratory differences, which are explained in the source reference by slight differences in the powder preparation. Since we used only material prepared at PSI, we discarded the specific surface areas determined at Studsvik, relying only on the PSI determinations. The latter indicate an uncertainty of ~ ±10 % for the surface area of the SON68 glass powders. For the MW glass powders a similar uncertainty of ~ ±10 % results from the reproducibility of the stereoscopic analyses, but if the higher numbers derived from BET measurements are taken into account, the uncertainty increases to ~ ±30 %. These figures were used to calculate the overall uncertainty of $NL(B)$ and $NL(Li)$ values and then the weighted regression, used to determine the long-term rate (Table A1, Appendix A). A

conservative surface area uncertainty of ±30 % was selected to derive the upper limit of the long-term rate for the MW glass.

b) uncertainties deriving from variations of the exposed surface area due to the dissolution of the glass: As the glass corrodes, the original surface is destroyed and the reaction proceeds on a constantly receding front. The decrease in surface area as a function of reaction progress was estimated with the help of a simple geometrical model (see section B.2) and was accounted for in the calculation of $NL(B)$ and $NL(Li)$ values for SON68.

B.2 Variation of exposed surface area with reaction progress

The change in surface area as a function of reaction progress is estimated with the help of a simple model based on the following assumptions:

a) The alteration layer is sufficiently porous to guarantee 100% accessibility to the fresh glass.

b) The glass grains are equally sized and spherical.

c) Corrosion acts evenly, so that the size of the grains decreases while the spherical geometry is conserved.

The first step is to express the initial mass of glass, m_0 [kg], as a function of grain radius r_0 [m], glass density ρ [kg m^{-3}] and the number of grains, ν [-]:

$$m_0 = \rho \frac{4}{3} \pi r_0^3 \nu . \qquad \text{(B1)}$$

The total initial surface area is given by:

$$S_0 = \psi_0 \, m_0 = \nu 4\pi r_0^2 \qquad \text{(B2)}$$

where ψ_0 [m^2 kg^{-1}] is the initial specific surface area of the glass. Solving Eq. (B1) for ν and substituting into Eq. (B2) yields:

$$r_0 = \frac{3}{\psi_0 \rho} = \frac{3}{1.2 \times 10^6 \, m^2 kg^{-1} \; 2.7 \times 10^3 \, kg \, m^{-3}} = 37 \mu m \qquad \text{(B3)}$$

This figure falls at the lower end of, but still within, the grain size range ($2r_0$ = 71-160 μm) determined by sieving the glass powders. This range corresponds to specific surface areas between 0.014 and 0.03 $m^2\ g^{-1}$, matching the values inferred through stereoscopic analyses (~ 0.03 $m^2\ g^{-1}$). The mass of unaltered glass, m [kg], at any reaction time is simply the difference between the initial amount of glass, m_0 and the amount reacted, m_r [kg]:

$$m = m_0 - m_r \tag{B4}$$

The latter quantity can be expressed as a function of the actual concentration of a congruently dissolving element in solution (B, Li) and of the solution volume, taking account of the losses due to previous samplings:

$$m_r = \frac{[B]_n\left(V_0 - (n-1)\Delta V\right)}{f_B} + \frac{\Delta V}{f_B}\sum_{i=1}^{n-1}[B]_i \tag{B5}$$

where ΔV is the sampling volume (10 mL) and *n* is the number of sampled ΔV volumes (*n*=1 corresponds to the first sampling). The first term gives the net amount of dissolved glass present in the reaction vessel before the n^{th} solution sample is taken; the second term gives the amount of dissolved glass removed from the reaction vessel due to previous samplings (1,2…,*n*-1). The mass of unaltered glass is, by analogy with Eq. (B1):

$$m = \rho\frac{4}{3}\pi\, r^3\, \nu \tag{B6}$$

Dividing Eq. (B6) by Eq. (B1) and rearranging one obtains:

$$r = r_0\sqrt[3]{\frac{m}{m_0}} = r_0\sqrt[3]{\frac{m_0 - m_r}{m_0}} \tag{B7}$$

Considering that the cumulative mass loss (m_r) due to the corrosion of the MW glass over 5 years is about 7.3 g and given an initial mass of 24 g, the radius of a spherical grain is reduced from 37 to ~33 μm (~10% of the initial radius). For

the SON68 glass (m_r ~ 1 g), the sphere radius is reduced only by 2%. The corresponding fractional decrease in surface area is given by:

$$\frac{S}{S_0} = \frac{r^2}{r_0^2} = \left(1 - \frac{m_r}{m_0}\right)^{2/3} \qquad \text{(B8)}$$

where S [m^2] is the surface area of unaltered glass after the amount m_r of pristine glass has reacted. For the MW glass, the calculated decrease in surface area is about 22 %, while for the SON68 glass the decrease is ~ 2%.

B.3 Variation of (S/V) for the calculation of normalised mass losses

During the experiments 11 solution aliquots were sampled, corresponding to a reduction of the initial solution volume by 18 %. This volume reduction compensates quite exactly the decrease in surface area estimated for the MW glass, so that the correction factor for the (S/V) term was close to unity. For the SON68 glass, however, the loss of solution due to the repeated sampling implies that the (S/V) ratio increased from 1200 to ~ 1400 m^{-1} in the course of the experiments. The calculated (S/V) values as a function of time are listed in Table C9, Appendix C. These values were used in calculating $NL(i)$ values.

B.4 Variation of specific surface area

Finally, the change in specific surface area is evaluated. The ratio of specific surface area to the initial value at any reaction progress can be calculated for the geometrical model developed above by combining Eqs. (B2), (B4) and (B8):

$$\frac{\psi}{\psi_0} = \frac{S}{\psi_0 m} = \frac{m_0\left(1 - \frac{m_r}{m_0}\right)^{2/3}}{m_0 - m_r} \qquad \text{(B9)}$$

For the MW glass an increase of ψ by 12 % is calculated (using m_r = 7.3 g and m_0 = 24 g) for the elapsed reaction time. For the SON68 glass the variation is negligible.

APPENDIX C: EXPERIMENTAL AND CALCULATED DATA

Table C1: Measured B concentrations [mg/L] in sampled solutions, MW glass.

t [d]	#1	#2	#3	#4	#5
0	0	0	0	0	0
28	393	368	420	419	376
91	439	440	486	517	445
365	507	507	536	579	502
548	540	534	568	611	540
730	553	545	570	601	534
1095	560	550	577	607	540
1460	555	549	576	602	539
1946	625	625	645	675	595
1983	588	589	625	629	596
2078	627	-	-	-	-
3070	-	672	692	731	667
3650	-	665	690	722	663

Table C2: Measured B concentrations [mg/L] in sampled solutions, SON68 glass.

t [d]	#6	#7	#8	#9	#10
0	0.0	0.0	0.0	0.0	0.0
28	53.0	49.1	50.8	49.2	50.7
91	57.3	54.6	57.8	56.6	54.4
365	60.5	58.5	59.7	60.0	60.5
548	64.9	62.5	62.9	61.4	63.9
730	63.0	63.0	64.0	62.0	62.0
1095	62.5	63.2	65.3	63.1	60.6
1460	61.2	64.8	64.9	63.8	59.9
1946	72.5	70.0	74.0	74.5	70.0
1983	75.2	70.7	72.8	72.0	73.3
2078	72.5	-	-	-	-
3070	-	86.8	82.5	82.1	81.1
3650	-	81.2	83.0	84.9	88.5

Table C3: Measured Li concentrations [mg/L] in sampled solutions, MW glass.

t [d]	#1	#2	#3	#4	#5
0	0	0	0	0	0
28	118	116	132	119	114
91	135	134	140	138	134
365	151	154	153	156	152
548	159	158	166	166	154
730	161	160	164	162	160
1095	161	160	165	164	163
1460	165	161	167	164	160
1946	174	166	169	168	160
1983	174	176	179	176	173
2078	179	-	-	-	-
3070	-	192	197	194	197
3650	-	194	197	189	192

Table C4: Measured Li concentrations [mg/L] in sampled solutions, SON68 glass.

t [d]	#6	#7	#8	#9	#10
0	0.0	0.0	0.0	0.0	0.0
28	12.0	11.8	11.6	10.9	11.4
91	12.7	12.2	13.1	12.8	12.2
365	14.1	13.8	13.7	13.9	14.2
548	15.4	14.6	15.0	13.9	14.8
730	14.8	14.4	15.2	14.8	14.4
1095	14.7	14.3	15.3	15.3	13.9
1460	14.7	14.5	15.0	15.0	14.2
1946	17.3	16.9	17.9	16.8	16.4
1983	17.7	17.8	17.0	17.2	17.2
2078	18.3	-	-	-	-
3070	-	19.8	19.4	19.0	19.1
3650	-	18.0	18.3	18.3	19.4

Table C5: Calculated boron normalised mass losses, $NL(B)$ [g m^{-2}] for MW glass.

(a) assuming constant S/V (1200 m^{-1})

t [d]	#1	#2	#3	#4	#5
0	0.00	0.00	0.00	0.00	0.00
28	6.53	6.11	6.98	6.96	6.25
91	7.29	7.31	8.07	8.59	7.39
365	8.42	8.42	8.90	9.62	8.34
548	8.97	8.87	9.44	10.15	8.97
730	9.19	9.05	9.47	9.98	8.87
1095	9.30	9.14	9.59	10.08	8.97
1460	9.22	9.12	9.57	10.00	8.95
1946	10.38	10.38	10.72	11.21	9.89
1983	9.77	9.79	10.38	10.45	9.90
2078	10.42	0.00	0.00	0.00	0.00
3070	0.00	11.72	11.99	12.70	11.61
3650	0.00	11.59	11.96	12.53	11.54

(b) corrected for variation of S/V

t [d]	#1	#2	#3	#4	#5
0	0.00	0.00	0.00	0.00	0.00
28	6.53	6.11	6.98	6.96	6.25
91	7.39	7.46	8.21	8.79	7.54
365	8.68	8.73	9.16	9.97	8.62
548	9.31	9.25	9.77	10.58	9.34
730	9.56	9.45	9.81	10.39	9.23
1095	9.69	9.55	9.94	10.50	9.34
1460	9.59	9.53	9.92	10.41	9.32
1946	10.86	10.91	11.17	11.73	10.34
1983	10.18	10.25	10.80	10.89	10.36
2078	10.87	-	-	-	-
3070	-	11.72	11.99	12.70	11.61
3650	-	11.59	11.96	12.53	11.54

Table C6: Calculated boron normalised mass losses, $NL(B)$ [g m^{-2}] for SON68 glass, corrected for variation in S/V.

t [d]	#6	#7	#8	#9	#10
0	0.00	0.00	0.00	0.00	0.00
28	1.01	0.94	0.97	0.94	0.97
91	1.10	1.04	1.10	1.08	1.04
365	1.15	1.12	1.14	1.14	1.15
548	1.23	1.19	1.20	1.17	1.21
730	1.20	1.20	1.22	1.18	1.18
1095	1.19	1.20	1.24	1.20	1.16
1460	1.17	1.23	1.23	1.21	1.14
1946	1.36	1.32	1.39	1.39	1.31
1983	1.41	1.33	1.37	1.35	1.37
2078	1.36	-	-	-	-
3070	-	1.59	1.52	1.52	1.50
3650	-	1.50	1.53	1.56	1.61

Table C7: Calculated lithium normalised mass losses, $NL(Li)$ [g m^{-2}] for MW glass.

(a) assuming constant S/V (1200 m^{-1})

t [d]	#1	#2	#3	#4	#5
0	0.00	0.00	0.00	0.00	0.00
28	5.59	5.49	6.25	5.63	5.40
91	6.39	6.34	6.63	6.53	6.34
365	7.15	7.29	7.24	7.39	7.20
548	7.53	7.48	7.86	7.86	7.29
730	7.62	7.58	7.77	7.67	7.58
1095	7.62	7.58	7.81	7.77	7.72
1460	7.81	7.62	7.91	7.77	7.58
1946	8.24	7.86	7.98	7.95	7.58
1983	8.24	8.33	8.48	8.33	8.19
2078	8.48	0.00	0.00	0.00	0.00
3070	0.00	9.50	9.67	9.59	9.76
3650	0.00	9.60	9.67	9.33	9.51

(b) corrected for variation of S/V

t [d]	#1	#2	#3	#4	#5
0	0.00	0.00	0.00	0.00	0.00
28	5.59	5.49	6.25	5.63	5.40
91	6.49	6.45	6.68	6.65	6.46
365	7.36	7.53	7.38	7.62	7.43
548	7.79	7.75	8.09	8.16	7.54
730	7.90	7.86	7.98	7.95	7.87
1095	7.90	7.86	8.03	8.05	8.03
1460	8.11	7.91	8.14	8.05	7.87
1946	8.58	8.17	8.21	8.26	7.87
1983	8.58	8.69	8.76	8.68	8.55
2078	8.83	-	-	-	-
3070	-	9.50	9.67	9.59	9.76
3650	-	9.60	9.67	9.33	9.51

Table C8: Calculated lithium normalised mass losses, $NL(Li)$ [g m^{-2}] for SON68 glass.

t [d]	#6	#7	#8	#9	#10
0	0.00	0.00	0.00	0.00	0.00
28	1.09	1.07	1.05	0.99	1.03
91	1.15	1.10	1.18	1.16	1.10
365	1.27	1.24	1.24	1.25	1.28
548	1.38	1.31	1.35	1.25	1.33
730	1.33	1.30	1.37	1.33	1.30
1095	1.32	1.29	1.37	1.37	1.26
1460	1.32	1.30	1.35	1.35	1.28
1946	1.53	1.50	1.58	1.49	1.45
1983	1.56	1.57	1.51	1.52	1.52
2078	1.61	-	-	-	-
3070	-	1.72	1.70	1.66	1.66
3650	-	1.59	1.61	1.61	1.69

Table C9: Solution volumes and calculated solid/liquid ratios, S/V.

t [d]	V [mL]	S/V [m^{-1}] (MW)	S/V [m^{-1}] (SON68)
0	600	1200	1200
28	590	1066	1220
91	580	1053	1241
365	570	1042	1263
548	560	1048	1286
730	550	1062	1309
1095	540	1080	1333
1460	530	1101	1358
1946	520	1087	1385
1983	510	1125	1412
2078	500	1130	1440
3070	500	1109	1440
3650	490	1135	1469

Table C10: Silica concentrations [mg/L] measured in MW glass solutions.

t [d]	#1	#2	#3	#4	#5
0	0	0	0	0	0
28	159	156	149	88	156
91	142	144	142	136	145
365	157	158	154	151	158
548	132	135	130	127	130
730	112	112	106	104	109
1095	98	100	90	91	88
1460	86	86	79	77	77
1946	140	140	135	134	135
1983	127	128	121	123	126
2078	98	-	-	-	-
3070	-	92	91	88	92
3650	-	91	85	83	90

Table C11: Silica concentrations [mg/L] measured in SON68 glass solutions.

t [d]	#6	#7	#8	#9	#10
0	-	-	-	-	-
28	89	87	88	86	86
91	96	95	96	93	93
365	104	102	103	102	101
548	87	85	87	86	85
730	83	79	82	80	79
1095	81	81	81	81	80
1460	80	79	80	80	81
1946	94	90	95	95	88
1983	75	71	90	87	73
2078	88	-	-	-	-
3070	-	85	86	89	81
3650	-	86	89	92	83